

Structural development of dynamically asymmetric polymer blends under uniaxial stretching

Hiroyuki Takeno,^{a*} Hiroki Uehara,^b Shozo Murakami,^c Mikihiro Takenaka,^d Myung Im Kim,^d Naotsugu Nagasawa^e and Sono Sasaki^f

^aDepartment of Biological and Chemical Engineering, Faculty of Engineering, Gunma University, Gunma 376-8515, Japan, ^bDepartment of Material Engineering, Faculty of Engineering, Gunma University, Gunma 376-8515, Japan, ^cHeian Jogakuin University, Osaka 569-1092, Japan, ^dDepartment of Polymer Chemistry, Graduate School of Engineering, Kyoto University, Kyoto 606-8501, Japan, ^eJapan Atomic Energy Agency, Takasaki, Gunma 370-1292, Japan, and ^fSPRING-8/JASRI, Hyogo 679-5198, Japan. Correspondence e-mail: takeno@bce.gunma-u.ac.jp

The time-resolved small-angle X-ray scattering technique was used to investigate the structural change during uniaxial stretching of dynamically asymmetric polymer blends irradiated by an electron beam. The concentration fluctuations were enhanced by stretching and became large in particular along the direction of deformation. In the early stages of the stretch-induced enhancement of concentration fluctuations, the growth rate of their q -Fourier mode was found to have a maximum at a certain value of q [$= (4\pi/\lambda)\sin(\theta/2)$, where θ and λ are the scattering angle and the wavelength of the X-rays, respectively]. A dominant mode in the enhancement of concentration fluctuations exists in the initial stage, like the early stage of spinodal decomposition for fluid mixtures. The viscoelastic effects of the growth rate were taken into consideration, so that for blends irradiated by an electron beam, elastic effects are found to significantly suppress the growth rate of concentration fluctuations at small wavenumbers.

© 2007 International Union of Crystallography
Printed in Singapore – all rights reserved

1. Introduction

A large number of intriguing phenomena have been observed for binary mixtures with dynamical asymmetry between two constituent components such as polymer solutions or polymer blends with a large difference in glass transition temperatures: viscoelastic phase separation (Tanaka, 1993, 1994, 1996; Takenaka *et al.*, 2002), shear-induced enhancement of concentration fluctuations (Dixon *et al.*, 1992; Hashimoto & Fujioka, 1991; Kume *et al.*, 1997) and so forth. The key concept of these phenomena is the dynamical coupling between stress and diffusion (Doi & Onuki, 1992). In this concept, the concentration fluctuations generate a local stress and the stress can influence spatial inhomogeneities of concentration through the coupling. Experimentally, many of these studies have so far been made on structural change under shear; for example numerous efforts have been devoted to the investigation of a unique anisotropic structure under shear, *i.e.* the butterfly pattern. (Dixon *et al.*, 1992; Hashimoto & Fujioka, 1991; Kume *et al.*, 1997; Koizumi, 2003).

On the other hand, for mixtures of short deuterated polystyrene (PS) chains dispersed in very long normal PS chains or in rubbers, structural studies during relaxation after stretching have been extensively investigated using small-angle neutron scattering (SANS) by Bastide *et al.* (Bastide *et al.*, 1988, 1990; Boue *et al.*, 1991; Zielinski *et al.*, 1992; Ramzi *et al.*, 1995). In their studies, an elliptical pattern was observed for short durations of relaxation after stretching, while a butterfly pattern was observed for long durations.

In this study, we investigated the structural development during uniaxial stretching at constant speed by means of small-angle X-ray scattering for miscible polymer blends with a large difference in glass transition temperatures (T_g), some of which were irradiated by an

electron beam. In particular, we concentrated upon the structural development near the T_g of the blend, where the difference in mobilities between two constituent components becomes very large. We shall discuss the time evolution of concentration fluctuations enhanced by stretching.

2. Experimental

2.1. Sample preparation and characteristics

In this study, we used a miscible blend of poly(2-chlorostyrene) (P2CS) and poly(vinyl methyl ether) (PVME), which have a large difference in glass transition temperatures ($\Delta T_g \simeq 155$ K). Both P2CS and PVME were purchased from Scientific Polymer Products. P2CS has a number-average molecular weight M_n of 30 000 and a molecular weight distribution M_w/M_n of 1.74 and PVME has $M_n = 44$ 000 and $M_w/M_n = 1.92$, where M_w represents the weight-averaged molecular weight. These values were obtained by gel permeation chromatography (GPC). Blends with a composition of 50/50 wt% were dissolved in benzene. The solution was freeze-dried and then annealed at *ca* 373 K for 2 days. Afterwards, the samples were melt-pressed at 373 K. The glass transition temperature of blends with 50/50 wt% is 292 K according to the literature (Urakawa *et al.*, 2001). Some blends were irradiated by an electron beam accelerator (3 MeV, 25 mA) with an acceleration energy of 2 MeV, a beam current 1 mA, and a dose rate of 10 kGy per pass. The irradiation with the electron beam was performed at the Japan Atomic Energy Agency in Takasaki. These blends have a lower critical solution temperature (LCST). The cloud points of the blends without irradiation, irradiated with 50 kGy and with 100 kGy are 432 ± 1 , 426 ± 1

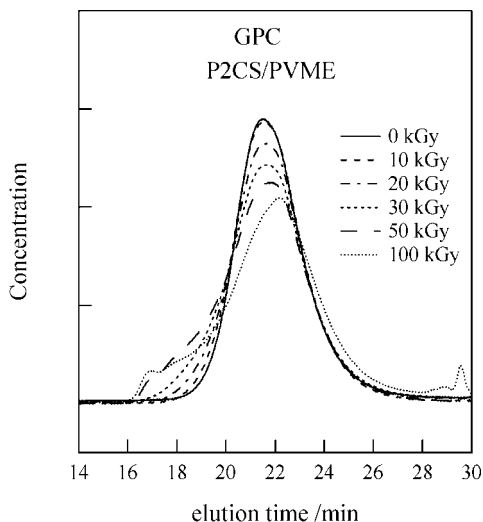


Figure 1
GPC results for blends irradiated with different doses.

and 429 ± 2 K, respectively. Mean-field spinodal temperatures estimated from scattering experiments in the single-phase state for blends without irradiation and irradiated with 100 kGy are 429.6 and 427.7 K, respectively. The Flory–Huggins interaction parameter χ for the blend without irradiation is -0.0462 at 315 K (Takeno *et al.*, unpublished data: the χ parameter was obtained by fitting of a theoretical equation based upon a random-phase approximation to the SAXS data).

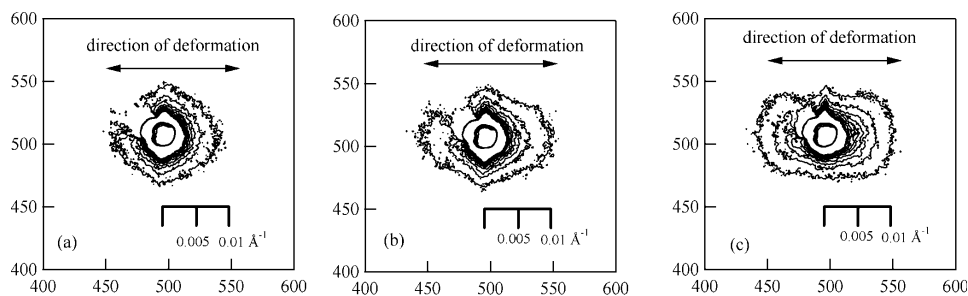


Figure 2
Two-dimensional SAXS patterns for the blend irradiated with 50 kGy during uniaxial stretching at 108 s (a), 156 s (b) and 228 s (c).

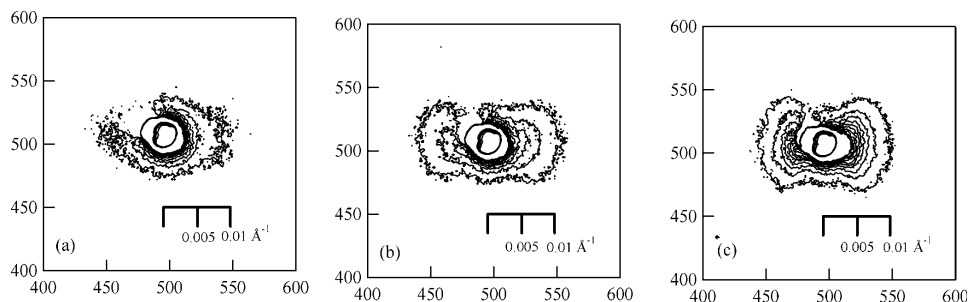


Figure 3
Two-dimensional SAXS patterns for the blend irradiated with 100 kGy during uniaxial stretching at 108 s (a), 168 s (b) and 288 s (c).

Table 1
Parameters estimated by fitting to the experimental data.

Sample	A ($\text{\AA}^2 \text{s}^{-1}$)	B ($\text{\AA}^4 \text{s}^{-1}$)	ξ_{ve} (\AA)
0 kGy	5.3×10^2	-4.0×10^6	164
50 kGy	6.0×10^2	-3.6×10^6	217
100 kGy	1.1×10^3	-8.0×10^6	251

2.2. Characteristics of irradiated samples

GPC measurements were carried out to investigate the properties of the irradiated blends. Moreover, we estimated the gel fraction w_g by weighing the insoluble sample remaining after dissolving the sample in toluene using w_g (%) = $W/W_0 \times 100$, where W and W_0 are the weight of the dried insoluble sample and the weight of the sample before dissolving it in the solvent, respectively. Consequently, the gel fractions were 1.0 and 1.4 wt% for the samples dosed with 50 kGy and 100 kGy, respectively. Thus, the irradiated blends are closer to melts containing long chains than rubber. Therefore the observations under deformation are not made at equilibrium, because the elastic energy provided by the deformation is dissipated with time.

2.3. Small-angle X-ray scattering

We followed the structural development during uniaxial stretching at a constant speed (24 mm min^{-1}) by time-resolved small-angle X-ray scattering (SAXS) measurements, which were carried out using the beamline BL40B2 at the synchrotron radiation facility SPring-8 in Harima, Japan. The details of the stretching machine for SAXS measurements have been described elsewhere (Murakami, 2000). The machine allowed us to carry out simultaneous measurements of SAXS and stress–strain data. The data were corrected for air scattering and transmittance and then sector-averaged over an angular

sector of 20° in the directions parallel and perpendicular to stretching to obtain the scattering intensity as a function of the modulus of the scattering vector q defined by $q = (4\pi/\lambda) \sin(\theta/2)$, where λ and θ are the wavelength of the X-rays and the scattering angle, respectively. The change of sample thickness during the stretching experiments was calculated on the basis of the assumption that the volume of the sample is unchanged under deformation. The change of the transmittance arising from the change of the sample thickness was also taken into consideration for data correction. The experiments were carried out at 313 K, at which temperature the blends are in a single-phase state in quiescence.

3. Results and discussion

3.1. Time-evolution of concentration fluctuations during uniaxial stretching

Fig. 1 presents the GPC results for the blends irradiated at different doses. There is almost no difference between the blend that was not irradiated and the blend irradiated with a dose of 10 kGy, while for the blends irradiated

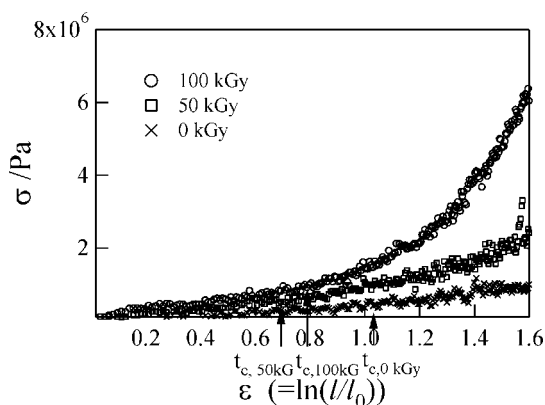


Figure 4
Stress versus strain curves for various blends.

with doses between 20 and 50 kGy the main peak decreases with increasing radiation dose and there is a broad increase of the signal in the range of low elution time, *i.e.*, high molecular weight, while there is no change in the range of high elution time (low molecular weight). The larger the radiation dose, the larger the increase of the signal at the low elution times. This result shows that there is only crosslinking in this range of doses and no chain scission. The GPC behavior is very similar to that of neat PVME irradiated by an electron beam (Liu *et al.*, 1994). Therefore, the crosslinking arising from electron irradiation comes from the PVME component. On the other hand, the curve for the blend irradiated with 100 kGy has a small peak at an elution time of 16.8 min, which corresponds to a molecular weight of *ca* 1×10^6 , while there is a slight increase in higher elution time (low molecular weight) and very small peak at 29.5 min corresponding to molecular weight of 540. Thus, for the blend irradiated with 100 kGy

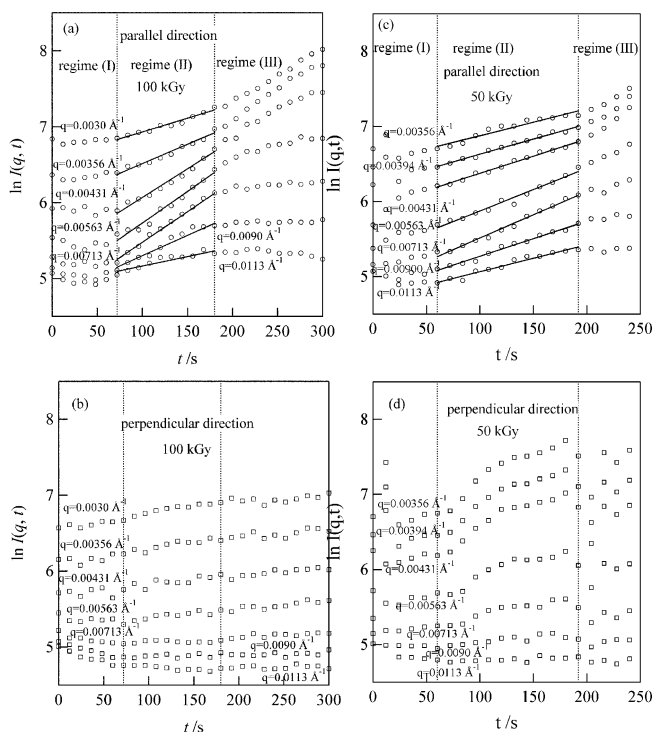


Figure 6
Plot of $\ln I(q, t)$ in the parallel and perpendicular directions against time at various q values for the blends irradiated with 100 kGy (a, b) and 50 kGy (c, d).

both crosslinking and chain scission take place on electron irradiation.

Fig. 2 shows two-dimensional SAXS patterns at 313 K for the blend irradiated with a dose of 50 kGy at 108 s (a), 156 s (b) and 228 s (c) after the onset of stretching. Unfortunately, excess scattering arising from the direct beam remains at the upper left even after background subtraction.

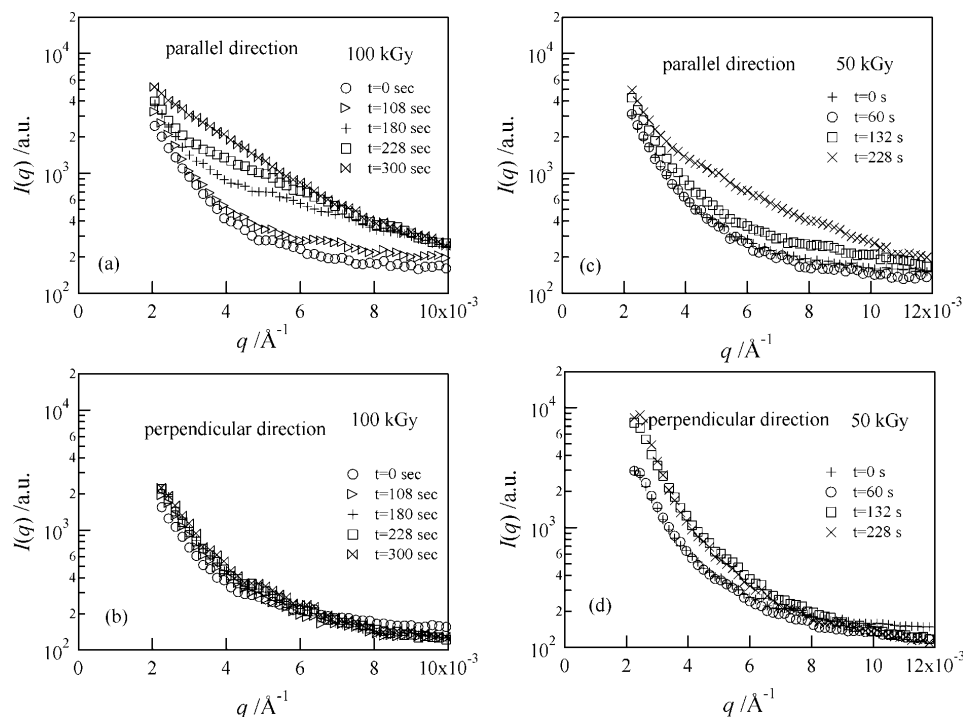


Figure 5
Scattering profiles in the directions parallel and perpendicular to stretching for the blends irradiated with 100 kGy (a, b) and 50 kGy (c, d) at different times.

In the analysis below, the excess scattering was excluded. The measurement temperature is between the T_g of P2CS (402 K) and that of PVME (247 K) (Urakawa *et al.*, 2001), where the intrinsic mobility of each component is expected to be quite different, and larger than the glass transition temperature of the blend (292 K; Urakawa *et al.*, 2001). As shown in Fig. 2(a), the two-dimensional scattering pattern becomes a little anisotropic a short time after stretching but the intensity becomes larger along both the parallel and perpendicular directions, which is similar to the ‘lozenge pattern’ observed by Boue *et al.* (1991) for a mixture of short deuterated PS chains dispersed in a PS network. With further stretching, the scattering intensity in the parallel direction becomes larger in comparison with that in the perpendicular direction and the pattern approaches a butterfly pattern. Boue *et al.* attributed the lozenge pattern to a

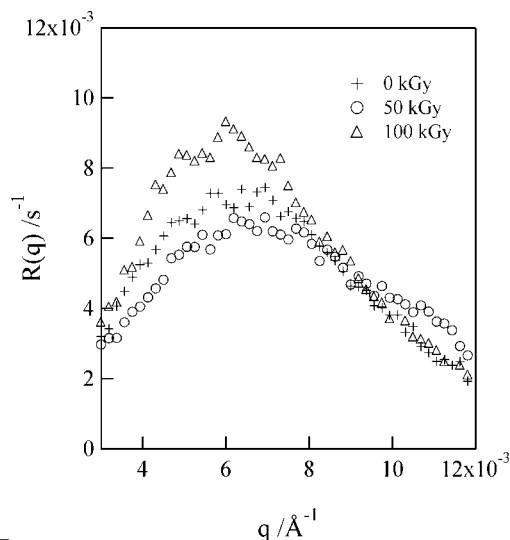


Figure 7
Plot of $R(q)$ versus q for various blends.

combination of the classical elliptical scattering with a butterfly scattering. In another paper, they observed a structural change from elliptic into butterfly scattering with an increase of the duration of relaxation. The characteristic time for the butterfly pattern was considered to be comparable to the terminal time for the polymer chain. Our scattering behavior is also similar to their results, *i.e.*, the butterfly pattern becomes pronounced with increase of the stretching time. For our blend we obtain a terminal time of 110 s from the literature value of the terminal time for a PS/PVME blend (Pathak *et al.*, 1999), the molecular weight and the difference between T_g and 313 K. On the other hand, for the more strongly irradiated blend the butterfly effect becomes stronger and the lozenge is not observed clearly (Fig. 3). As shown in Fig. 4, the value of the stress measured simultaneously during SAXS experiments for the blend irradiated with 100 kGy is larger than that for the blend irradiated with 50 kGy because of the increase of crosslinking, although for the former chain scission also takes place (Fig. 1). Similar behavior was reported by Boue *et al.*, *i.e.*, no lozenges were observed for more crosslinked samples. Thus, our scattering pattern is qualitatively similar to those in earlier work. However, it is important to notice that the phenomena reported by Boue *et al.* arise from heterogeneities in crosslinked chains, while the phenomena seen here may have characteristics of the phase separation type. On the other hand, Erukhimovich *et al.* (1998) reported that for a blend of crosslinked PS and PVME a butterfly pattern was observed under uniaxial stretching, although no pictures of the butterfly pattern were shown in the paper. They claimed that a blend of two polymers with a large difference in T_g values shows microphase separation and such microphases lead to butterfly patterns under stretching. At least for our blend without irradiation, the scattering behavior before deformation did not show proof of such microphases. Fig. 5 shows the scattering profiles in the directions parallel and perpendicular to stretching at different times for the irradiated blends. For the blend irradiated with 100 kGy, the concentration fluctuations in the parallel direction were remarkably enhanced by stretching in comparison with those in the perpendicular direction. On the other hand, for the blend irradiated with 50 kGy, in the small- q region the scattering intensity in the perpendicular direction becomes larger, while in the high- q region it becomes larger in the parallel direction.

Here we shall investigate the q dependence of the time evolution of the concentration fluctuations. In Fig. 6, we show the time evolu-

tion of the scattering intensity at a fixed q , $I(q, t)$, in the parallel and perpendicular directions. The scattering intensity in the perpendicular direction for the blend dosed with 100 kGy hardly changes with time, while it increases significantly with time in the small- q region for the blend dosed with 50 kGy. (However, if we take a careful look at the figure, the perpendicular intensity for the blend dosed with 100 kGy also increases slightly with time.) The time evolution of the scattering intensity in the parallel direction can be divided into three regimes. The scattering intensity shows almost no change until a critical time (t_c) (regime I). That is, until t_c stretch-induced enhancement of the concentration fluctuations does not take place. At times larger than t_c , the scattering intensity starts to increase. In the cases of the blends irradiated with 50 and 100 kGy, t_c corresponds to about 60 and 72 s, respectively. The extension ratio of the sample at these times is *ca* 2. Moreover, the values of t_c are close to the estimated terminal time. In this regime, the logarithm of the scattering intensity has a linear relation with t (regime II). As seen from the figure, the slope depends significantly on q . Afterwards, the scattering intensity deviates from the linear relation upwards for small q or downwards for high q (regime III).

For the scattering behavior in regime (II), *i.e.*, at the initial stage of stretch-induced enhancement of concentration fluctuations, we shall describe the time evolution of the scattering intensity in the form

$$I(q, t) = I_0 \exp[R(q)t], \quad (1)$$

where $R(q)$ is the growth rate of the q -Fourier mode of the concentration fluctuations. We estimated $R(q)$ from the slope of the plot in Fig. 6. The solid lines represent the fitted lines. In Fig. 7, we present the plot of $R(q)$ obtained with this procedure against q for three blends irradiated with different doses. The $R(q)$ values obtained have a maximum for all the samples. This result means that a dominant mode in the enhancement of concentration fluctuations induced by uniaxial stretching exists, which is similar to the enhancement of concentration fluctuations at the early stage of spinodal decomposition represented by Cahn's linearized theory (Cahn, 1965).

3.2. Effect of crosslinking on the growth rate of concentration fluctuations

According to Helfand & Fredrickson (1989), Milner (1993) and Doi & Onuki (1992), the dynamical equation for concentration fluctuations which takes into consideration the dynamical coupling effect between stress and diffusion is

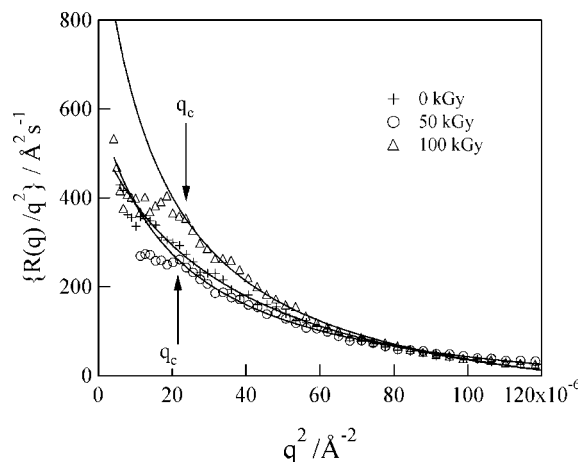


Figure 8
Plot of $\{R(q)/q^2\}$ versus q^2 for various blends.

$$\left(\frac{\partial}{\partial t} + \mathbf{v} \cdot \nabla\right)\phi = \nabla \cdot L \left[\nabla \frac{\delta F}{\delta \phi} - \alpha \cdot \nabla \boldsymbol{\sigma}^{(n)} \right], \quad (2)$$

where \mathbf{v} is the average velocity of the polymers, F is the free energy functional in the Ginzburg–Landau scheme, α is a parameter which characterizes dynamical asymmetry, L is the Onsager kinetic coefficient and $\boldsymbol{\sigma}^{(n)}$ is the network stress tensor. To linear order, the Fourier transformation of equation (2) yields the following equation for the Fourier component ϕ_q (Onuki & Taniguchi, 1997):

$$\frac{\partial}{\partial t} \phi_q = -Lq^2(r_0 + Cq^2)\phi_q - L\alpha Z_q, \quad (3)$$

where Z_q is the Fourier component of

$$Z = \nabla \cdot \nabla \cdot \boldsymbol{\sigma}^{(n)}. \quad (4)$$

The first term on the right-hand side of equation (3) corresponds to the growth rate of concentration fluctuations in the absence of a dynamical coupling effect. r_0 and C are related to the free energy functional by

$$\frac{\delta F}{\delta \phi} = (r_0 - C\nabla^2)\delta\phi. \quad (5)$$

Considering uniaxial stretching along the x direction, we obtain

$$\frac{\partial}{\partial t} \phi_q = -L \left[q^2(r_0 + Cq^2) - \alpha \left(\frac{\partial \sigma_{xx}}{\partial \phi} q_x^2 - \frac{\partial \sigma_{yy}}{\partial \phi} q_y^2 - \frac{\partial \sigma_{zz}}{\partial \phi} q_z^2 \right) \right] \phi_q. \quad (6)$$

Thus, from equation (6) we consider the relaxation rate of the concentration fluctuations $\Gamma(q)$ under stretching, although in fact the stress term depends upon time to some degree:

$$\Gamma(q) = -R(q) = L \left[q^2(r_0 + Cq^2) - \alpha \left(\frac{\partial \sigma_{xx}}{\partial \phi} q_x^2 - \frac{\partial \sigma_{yy}}{\partial \phi} q_y^2 - \frac{\partial \sigma_{zz}}{\partial \phi} q_z^2 \right) \right]. \quad (7)$$

In polymeric systems, the Onsager kinetic coefficient has a q dependence (Pincus, 1981). In the context of the Flory–Huggins theory, r_0 and C are presented as follows (Binder, 1983): $r_0 = 1/N_A\phi_A + 1/N_B\phi_B - 2\chi$ and $C = a^2/18\phi_A\phi_B$, where ϕ_i denotes the volume fraction for component i ($i = A$ or B) with polymerization degree N_i , a and χ are the statistical segment length and the Flory–Huggins interaction parameter, respectively. In particular, for dynamically asymmetric systems even in the very small q range the coefficient depends upon q (Doi & Onuki, 1992; Takenaka *et al.*, 2002),

$$L(q) = \frac{L(0)}{1 + q^2\xi_{ve}^2}, \quad (8)$$

where ξ_{ve} represents the correlation length of viscoelastic effects, called the ‘viscoelastic length’, and usually has a value larger than the gyration radius of the polymer chains.

In Fig. 8 we show a plot of $R(q)/q^2$ versus q^2 . The plot shows downward curves for all the blends. We carried out a fitting to the data with $R(q)/q^2 = (A + Bq^2)/(1 + q^2\xi_{ve}^2)$ (A and B are q -independent constants) based upon the form of equations (7) and (8):

$$A = -L(0) \left(r_0 - \alpha \frac{\partial \sigma_{xx}}{\partial \phi} \right), \quad (9)$$

$$B = -L(0)C. \quad (10)$$

The fitted result is good over all the q range for the blend that was not irradiated by the electron beam, while the fitted curves for blends irradiated by the electron beam cannot describe the data well in the small- q region. The parameters obtained from the fit are summarized in Table 1.

First, we can qualitatively see that since $A > 0$ for all the blends, $r_0 - \alpha(\partial\sigma_{xx}/\partial\phi)$ is negative [$L(0)$ is positive in order to be physically meaningful]. The result suggests that the concentration fluctuations become unstable due to the stress term. The values of ξ_{ve} are large relative to the radius of gyration of the component polymers R_g (the values of R_g calculated assuming ideal chains are $R_{g, P2CS} = 40 \text{ \AA}$, $R_{g, PVME} = 75 \text{ \AA}$), reflecting viscoelastic effects. Irradiation is considered to affect r_0 , $L(0)$ and $\alpha(\partial\sigma_{xx}/\partial\phi)$, and is expected to be insensitive to C . In our blends, the LCST was decreased by crosslinking, *i.e.*, the system tended to promote phase separation and therefore $R(q)$ becomes larger due to the effect of r_0 . $L(0)$ decreases if it is dominated by crosslinking, while it increases in the case of chain scission. It is predicted that in the case of the blend irradiated with a dose of 50 kGy $R(q)$ becomes smaller due to the decrease of $L(0)$ arising from crosslinking in comparison with that of the blend that was not irradiated, while for the blend dosed with 100 kGy $R(q)$ becomes larger due to r_0 and/or the effect of chain scission. There is a critical wavenumber q_c below which the deviation from equations (7) and (8) takes place for the irradiated blends. The growth rate of concentration fluctuations for the irradiated blends was found to be suppressed in the small- q region relative to the prediction from equations (7) and (8).

According to Tanaka *et al.* (1973) and Onuki & Taniguchi (1997), in a system in which stress relaxation is very slow, such as a gel (in the gel limit), the growth rate of concentration fluctuations is presented in the following form (Tanaka *et al.*, 1973; Onuki, 1997):

$$-R(q) = Lq^2 \left(r_0 + \frac{4}{3}\alpha^2 G + Cq^2 \right), \quad (11)$$

with $L(q) \simeq L$, where G is the shear modulus. From equation (11), in the gel limit we notice that the growth rate tends to be suppressed by the effect of G . Since our irradiated blends are closer to long chains than to a gel, the stress is expected to relax with time. The stress with long relaxation time may be dominant in the small- q region. In such a case the system transiently behaves as gel only for small q . Therefore, it is expected that suppression of the growth rate took place particularly for small q . Thus, in the case of irradiated blends, we guess that in the high- q region the growth rate of the concentration fluctuations has a viscoelastic character, while in the small- q region the growth rate was suppressed by elastic effects due to crosslinking in the blends.

4. Conclusion

We investigated the time evolution of stretch-induced enhancement of concentration fluctuations for polymer blends weakly crosslinked by irradiation by an electron beam. The growth rate of the concentration fluctuations was found to have a peak at a particular q . A dominant mode of growth rate exists in the early stage of stretch-induced enhancement of concentration fluctuations. The effect of the crosslinking on the growth rate of concentration fluctuations appears in the small- q region.

We acknowledge Mr Mochizuki at Gunma University for helping with measurements of cloud points and gel fractions.

References

- Bastide, J., Buzier, M. & Boue, F. (1988). *Polymer Motions in Dense Systems*. Springer Proceedings in Physics, Vol. 29, pp. 112–120. Heidelberg: Springer.
 Bastide, J., Leibler, L. & Prost, J. (1990). *Macromolecules*, **23**, 1821–1825.
 Binder, K. (1983). *J. Chem. Phys.* **79**, 6387–6409.

- Boue, F., Bastide, J., Buzier, M., Lapp, A., Herz, J. & Vilgis, A. (1991). *Colloid Polym. Sci.* **269**, 195–216.
- Cahn, J. W. (1965). *J. Chem. Phys.* **42**, 93–99.
- Dixon, P. K., Pine, D. J. & Wu, X.-L. (1992). *Phys. Rev. Lett.* **68**, 2239–2243.
- Doi, M. & Onuki, A. (1992). *J. Phys. II (France)*, **2**, 1631–1656.
- Erukhimovich, I. Ya., Khokhlov, A. R., Vilgis, T. A., Ramzi, A. & Boue, F. (1998). *Comput. Theor. Polym. Sci.* **8**, 133–142.
- Hashimoto, T. & Fujioka, K. (1991). *J. Phys. Soc. Jpn.* **60**, 356–359.
- Helfand, E. & Fredrickson, G. H. (1989). *Phys. Rev. Lett.* **62**, 2468–2471.
- Koizumi, S. (2003). *J. Appl. Cryst.* **36**, 381–388.
- Kume, T., Hattori, T. & Hashimoto, T. (1997). *Macromolecules*, **30**, 427–434.
- Liu, X., Briber, R. M. & Bauer, B. J. (1994). *J. Polym. Sci.* **32**, 811–815.
- Milner, S. T. (1993). *Phys. Rev. E*, **48**, 3674–3691.
- Murakami, S. (2000). *Nippon Kagaku Kaishi*, **2**, 141–146.
- Onuki, A. (1997). *J. Phys. Condens. Matter*, **9**, 6119–6157.
- Onuki, A. & Taniguchi, T. (1997). *J. Chem. Phys.* **106**, 5761–5770.
- Pathak, J. A., Colby, R. H., Floudas, G. & Jerome, R. (1999). *Macromolecules*, **32**, 2553–2561.
- Pincus, M. (1981). *J. Chem. Phys.* **75**, 1996–2000.
- Ramzi, A., Zielinski, F., Bastide, J. & Boue, F. (1995). *Macromolecules*, **28**, 3570–3587.
- Takenaka, M., Takeno, H., Hasegawa, H., Saito, S., Hashimoto, T. & Nagao, M. (2002). *Phys. Rev. E*, **65**, 021806-1–021806-9.
- Tanaka, H. (1993). *Phys. Rev. Lett.* **71**, 3158–3161.
- Tanaka, H. (1994). *J. Chem. Phys.* **100**, 5323–5337.
- Tanaka, H. (1996). *Phys. Rev. Lett.* **76**, 787–790.
- Tanaka, T., Hocker, L. O. & Benedik, G. B. (1973). *J. Chem. Phys.* **59**, 5151–5159.
- Urakawa, O., Fuse, Y., Hori, H., Tran-Cong, Q. & Yano, O. (2001). *Polymer*, **42**, 765–773.
- Zielinski, F., Buzier, M., Lartigue, C., Bastide, J. & Boue, F. (1992). *Prog. Colloid. Polym. Sci.* **90**, 115–130.